공학석사학위논문

The Development of Multi-degree of Freedom Hand Musculoskeletal Model for Analyzing Muscle Activations of Hand Motion and Validation

손 움직임의 근육 활성도 분석을 위한 다자유도 손 근·골격 모델개발 및 검증

2016년 8월

서울대학교 대학원

기계항공공학부

최 우 성

Abstract

Biomechanics is an academic field that understands the biological system by mechanical principles. There have been progresses in the study of computer modeling and simulation for biomechanics. Especially, musculoskeletal models of lower extremity have been developed for analysis of gait motion. However, there has been little research about the musculoskeletal model of upper limbs for the simulation analysis. No validated model is provided in freely available simulation software and commercial simulation programs. The aim of this study was to develop a hand musculoskeletal model for biomechanical analysis about various and complicated hand motions using AnyBody Modeling System and validate the model. The skeletal hand model was created based on the anatomical data to implement degrees of freedom of hand. The musculoskeletal hand model included the hill-type muscle models which made hand movements. The origin and the insertion attachment points of the muscles were founded using an optimization method to create moment arms of muscles from cadaveric study. The distance between motion capture markers and virtual markers was compared to validate the skeletal model.

Muscles were validated through the comparison between the experimentally−measured moment arms of muscles and calculated moment arms of muscles in the musculoskeletal model. The developed hand musculoskeletal model could be used to analyze musculoskeletal diseases in the hand such as carpal tunnel syndrome. This study will help understanding of pathological causes and improving the pathological diagnosis.

Keywords: Musculoskeletal model, computer simulation, hand, motion capture, moment arm, validation

Student Number: 2014−22506

Table of Contents

List of Figures

Chapter 1

Introduction

Biomechanics is an academic field that understands the biological system by mechanical principles. Especially, in the biomechanical study of the muscles and skeleton units, kinematics and kinetics are major themes. Kinematics deals with only the movement and is not considered with respect to the forces exerted on the object. Kinetics is area to study the result of the force to change the movement of object. [1]

Biomechanical study has been used widely in an experimental analysis. The position and orientation of a body is recorded using cameras and the direction and magnitude of ground reaction force is measured by force plates. Surface EMG measurement devices is used to record the muscle activities. However, it has clear limitations to understand the kinematics and kinetics through the experiments. It is possible to measure the muscle force to make movements and difficult to know the muscle coordination. Although activities of muscle could be understood by measuring the EMG signals of muscles, it is impossible to know which muscles are activated to make motions. [2, 3]

In order to overcome the limitations above, there have been progresses in the study of computer modeling and simulation for biomechanics. [4] It has been believed that muscle coordination in neuro−musculoskeletal system could be seen through computer modeling and simulation. In fact, simulation studies have been actively conducted using musculo−skeletal model with progress of the performance of the computer. [5, 6] Improving the performance of the computer has made it possible to increase the complexity of the motions for simulation. Using the musculo−skeletal model with many degrees of freedom, biomechanical analysis of the motion similar to the actual motion is made possible. [7]

Through computer modeling and simulation study, the study of gait motion has been conducted actively. In particular, joint contact force and muscle force of lower extremity could be predicted, which could not be directly measured through the experiment. In order to perform the correct musculoskeletal simulation, there was a need for a skeleton model reflecting the anatomical data of a real human body. In a related study, various musculoskeletal models have been developed for the human motions. Especially, musculoskeletal models of lower extremity have been developed for analysis of gait motion. The development of models enables researchers to predict ground reaction forces and knee joint reaction forces. [8, 9, 10]

However, there is little biomechanical research about the musculoskeletal model of upper limbs. In fact, No validated model is provided in freely available simulation software and commercial simulation programs. There are limitations for using the existing upper extremity models offered in simulation programs. First, the models don't include intrinsic finger muscles for the complex motions, making it difficult to predict the exact biomechanical analysis of the various motions. Secondly, it is impossible for biomechanical researchers to use the musculoskeletal models, because a number of models have been developed internally and unreleased. [11]

Recently, the use of multi-touch tablets and smart phones is increasing in daily life. Using these devices requires finger and hand movements that could potentially be associated with muscular skeletal diseases. In fact, the prolonged use of smart devices has increased the disorder of the wrist and finger. However, there are little research that evaluates musculoskeletal disorders associated with repetitive finger movements.

The aim of this study was to develop a hand musculoskeletal model for biomechanical analysis about various and complicated hand motions and validate the model. Hand musculoskeletal model was configured using the human anatomy information and validated through comparison between experimental and modeled moment arms. The commercial software AnyBody Modeling System [12] (AnyBody Technology, Aalborg, Denmark), an inverse dynamics-based optimization solver, was used to develop the musculoskeletal model of the hand.

Chapter 2

Configuration of the hand model

2.1 Anatomy of the hand

2.1.1 Bones and joints of the hand

Hand is the distal part of the human arm located below the forearm and consists of wrist, metacarpal bones, and 5 fingers (Figure 1). Wrist is the joint between the forearm and the metacarpal bones and consists of eight carpal bones. Fingers contain some of the densest areas of nerve endings on the body and are the part associated with the sense of touch. Hand includes 27 bones which are 8 carpals, 5 metacarpal bones, and 14 phalangeal bones. 5 metacarpal bones connect the wrist and fingers. [13, 14]

Wrist consists of eight small bones and forms two lines horizontally. The proximal row of carpal bones articulates with forearm bones and the distal row is more rigid as its transverse arch move with the metacarpals. Wrist joint functions flex/extension and ab/adduction like a universal joint (2 DOFs). [15]

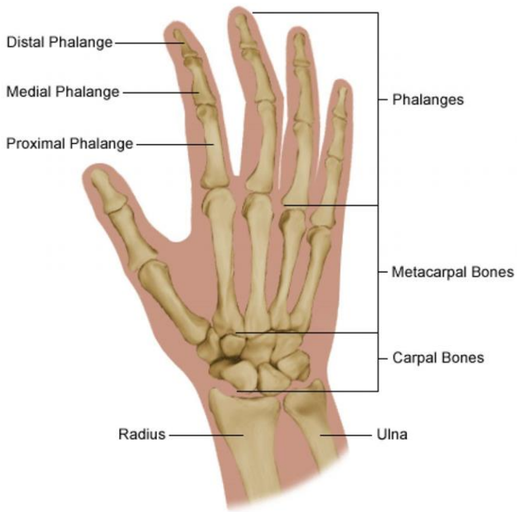

Figure 1. Skeleton of the hand

Metacarpal bones are long bones within the hand that are connected to the wrist bones and finger bones. They consist of 5 bones and each metacarpal bone is divided into base, body, and head from proximal part. Base of metacarpal bone articulates with distal row of wrist bone and head of metacarpal bone articulates with proximal phalanx in the finger bones.

The phalanges are the bones that make up the five fingers of the hand and consist of 14 bones. Only the first finger consists of two bones (proximal phalanx and distal phalanx) and the rest of fingers consist of three bones (proximal phalanx, intermediate phalanx, and distal phalanx).

The hand includes 20 joints providing 27 degrees of freedom. For the wrist joint, it connects the radius bone in forearm and the proximal carpal bones in the wrist. The carpometacarpal joints (CMC joint) are five joints in the wrist that articulate the distal row of carpal bones and the proximal bases of the five metacarpal bones. The metacarpophalangeal joints (MCP joint) refer to the joints between the metacarpal bones and the phalanges of the fingers. The heads of the metacarpals articulate with the base of the proximal phalanx of the fingers and thumb. For the thumb, it only consists of a proximal and distal phalanx, which means that there is just one interphalangeal joint (IP joint). The each finger of four fingers consists of three phalanx bones: proximal, middle, and distal. Therefore, there are two joints in the each finger. Proximal interphalangeal joint (PIP joint) connects the proximal and the intermediate phalanx. Distal interphalangeal joint (DIP joint) is connection between the intermediate and the distal phalanx.

2.1.2 Muscles of the hand

The muscles in the hand offer the driving force of the musculoskeletal system to generate hand motions. The muscles acting on the hand can be subdivided into two groups: the extrinsic and intrinsic muscle groups (Figure2) [16]. The origins of the extrinsic muscles are located on the forearm and they are connected to the tendons attached to the phalanges of the fingers. The extrinsic muscles control crude movements, and produce a forceful grip. The muscles are the long flexors and extensors. The flexors allow for the actual bending of the fingers. The primary function of the extensors is to straighten out the digits. But, the extensors are connected in a more complex way than the flexors.

The intrinsic muscles of the hand are located within the hand itself. They are responsible for the fine motor functions of the hand.

For the thumb, the intrinsic muscles can be divided into two groups: the thenar eminence and other muscles. The three muscles composing the thenar eminence are the abductor pollicis brevis, flexor pollicis brevis and opponens pollicis. The other two muscles that influences movement of the thumb are the adductor pollicis and the first dorsal interosseous muscle. The functions of the muscles are flexion, extension, adduction, abduction and opposition of the thumb. For the 4 fingers except thumb, there are three intrinsic muscles in each finger: the interossei muscles and the lumbrical muscle. They flex/extend and abduct/adduct the hand and fingers.

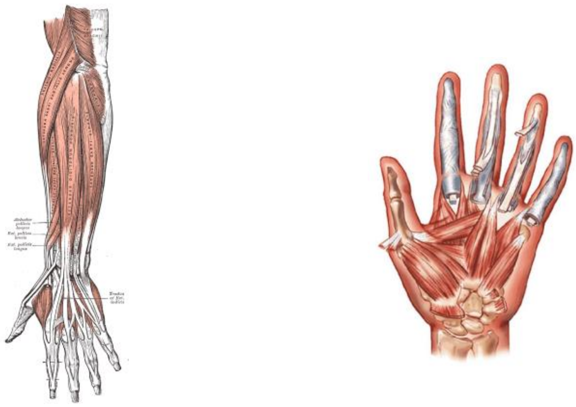

Figure 2 Extrinsic (Left) and intrinsic (Right) muscle of the hand

2.2 Musculoskeletal model of the hand

2.2.1 Base model

The musculoskeletal model of the hand was configured in the AnyBody Modeling System (AMS, AnyBody Technology, Aalborg, Denmark) to analyze the musculoskeletal system of the hand. AMS is a software system with an inverse dynamics based optimization solver. This software enables the biomechanical researchers to analyze joint reaction forces, body movements, and muscle forces. In the AMS software, each bone in the hand was modeled as a rigid single body to solve dynamic problems with multi degrees of freedom.

AMS, the commercial software, is based on a script language. This software has an advantage because the user could modify the existing model and develop the musculoskeletal model. There are musculoskeletal models to analyze the musculoskeletal system in the AMS. The models include both the upper limbs and lower limbs, and each body part of the models was constructed from the anatomical data of the different studies. In this research, the hand model was developed by modifying the Shoulder Arm Model provided in the AnyBody managed model repository (AMMR, version 1.6) of the AMS.

2.2.2 Joint configuration of the hand model

Hand is made up of 27bones, and 20 joints from wrist to the fingers. The hand bones were modeled as a single body in the Shoulder Arm Model. Detail hand model which consisted of 20 bones and increased degrees of freedom of the hand model can be obtained in AMS by changing the settings. However, joint configuration and DOF of this model was different from the anatomy of the hand. To configure the realistic musculoskeletal model, the configuration of the hand bones and joints was changed using the anatomical data of the hand. Joints of the hand were composed of a variety of mechanical joints based on the anatomical data.

CMC joints were composed of different mechanical joint for an each finger. Basically, CMC joint were universal joint which offered 2DOFs, flexion/extension and abduction/adduction. However, CMC joints of the index and middle finger were composed of fixed joint and joint movements were limited, because these joints had little motion based on anatomical research. [17]

MCP joint, which connected metacarpal bone and proximal phalanx, had 2DOFs (flexion/extension and abduction/adduction). 5 MCP joints all had same degree of freedom and consisted of universal joint (2DOFs). IP joint, which connected finger bones, had 1 DOF (flexion/extension), consisted of hinge joint.

2.2.3 Muscle modeling of the hand model

Researchers tried to find factors which affect the generation of the muscle force. In biomechanical analysis, Hill-type muscle model [18] has been used for the dynamic analysis of the musculoskeletal model. Hill-type muscle model consists of three mechanical elements to reflect the physiological characteristics of the muscle.

The model was constituted by a contractile element (CE) and two non-linear spring elements, one in series (SE) and another in parallel (PE). The factors used to characterize each muscle were maximum isometric force, optimal muscle fiber length, tendon slack length, maximum contraction velocity, and pennation angle. For all fingers, the following muscles were modeled: terminal extensor (TE), extensor slip (ES), radial band (RB), ulnar band (UB), dorsal interosseous or radial interosseous (RI), lumbricals (LU), palmar interosseous or ulnar interosseous (UI), flexor digitorum profundus (FDP), flexor digitorum superficialis (FDS) and extensor digitorum communis (EDC).

Chapter 3

Methods

3.1 Data acquisition

Motion capture experiment was conducted to obtain motion data from a subject. (Figure 3) One subject (age 28-year-old male, mass 85kg, height 181cm) participated in this study who was free of upper extremity musculoskeletal disorders (MSDs). 31 skin markers of 4mm-size were attached to different bony landmarks on right hand, forearm, elbow, upper arm and shoulder along with marker set of existing researches. [19] Motion data of right upper extremity were recorded using an optoelectronic motion capture system at 100Hz with 7 infrared video cameras. (Bonita B3, VICON, Oxford, UK) The motion capture system was synchronized with the recording software, Nexus (VICON, Oxford, UK). The motion data could be easily converted to the C3D file format using this software tool.

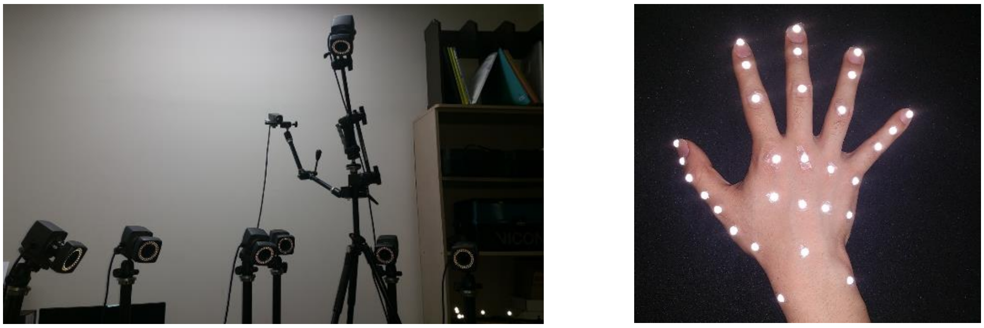

Figure 3. Motion capture environment and skin markers

Repetitive movements of each finger were recorded sequentially from the thumb to the little finger. Physiological hand motion started from a static posture to flexion/extension and abduction/adduction motions. Marker trajectories were filtered with a 4^{th} order zero−lag, low−pass Butterworth filter with a 4Hz cut−off frequency using MATLAB (Mathworks, Massachusetts, United States).

3.2 Scaling of the hand skeleton model

In order to analyze the biomechanical results about motions of the subject, the musculoskeletal model in AMS would be used. However, the size of musculoskeletal model should be adjusted to the size of the subject (Figure 4). In fact, to adjust size of the musculoskeletal model is possible by adjusting generalized parameters which are related to the size of body segments. Scaling is the process to minimize the distance between markers attached to the subject and virtual markers attached to the musculoskeletal model in AMS. Through parameter optimization sequence, parameters such as finger length and width were adjusted to fit the size of the subject. (Figure 5) [20]

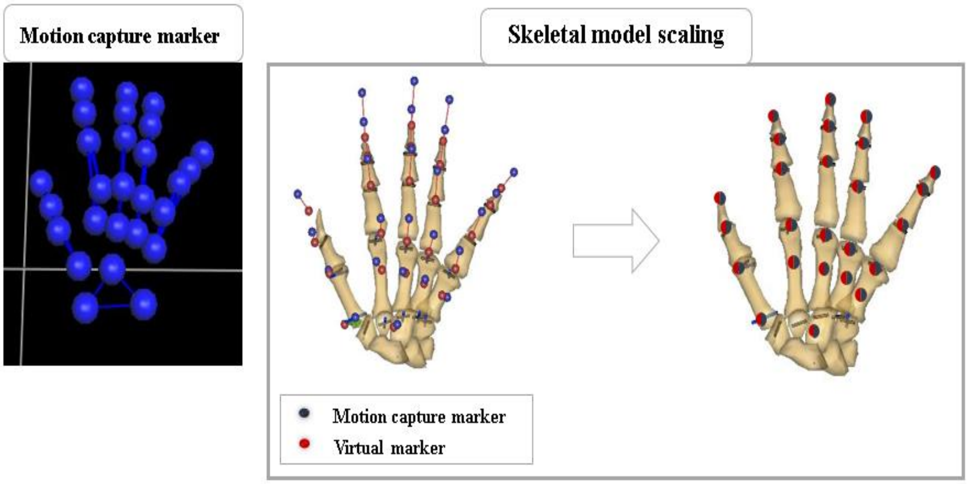

Figure 4. Motion capture marker and scaling process

This method [21] used the optimization method to close the distance between motion capture markers and the virtual markers attached to the musculoskeletal model. This method can be cast as the following objective function:

$$\begin{array}{ll} \min\limits_{q} \mathrm{G}(\psi(q,t)) & q \;: system\ coordinate \\ & t \;: time \\ subject\ to\ \phi(q,t) = 0 & \end{array}$$

$\mathrm{G}(\psi(q,t))$ is a function of the constraint equations that are allowed to be violated. $\phi(q,t)=0$ means the joint constraints to be fulfilled exactly. The motion capture marker and virtual marker belongs to $\mathrm{G}(\psi(q,t))$. To minimize objective function value, 3D points of segment surface were scaled by following scaling matrix. (Figure 5)

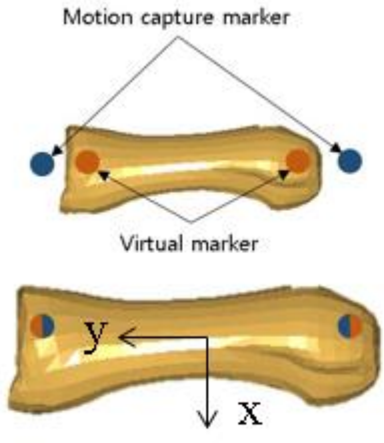

Figure 5. Optimization based scaling process

$$\text{Scaling matrix S} = \begin{bmatrix} S_{11} & 0 & 0 \\ 0 & S_{22} & 0 \\ 0 & 0 & S_{33} \end{bmatrix}$$

- $S_{11} = S_{33} = \sqrt{\frac{k_m}{k_L}} \quad , S_{22} = k_L$

- $K_m = \frac{m_1}{m_0}$ • $K_L = \frac{L_1}{L_0}$

S_{11}, S_{22}, and S_{33} are scaling factors for x, y, and z direction, respectively. S_{11} and S_{33} are $\sqrt{\frac{k_m}{k_L}}$ which reflects both the length and the mass of segment. S_{22} is the scaling factor of length direction and it reflects only the length of the segment. K_L and K_m are the rate of change before and after scaling of length and mass of the segment.

The scaled points could be expressed by following equation:

$$\text{Scaled point s} = \text{Sp} + \text{t (p : original point, t ; translation)}$$

Original points could be adjusted by the scaling matrix and translation.

3.3 Determination of muscle attachment point

There have been a number of different methods to validate the musculoskeletal model and system. Typically, 3 methods are used for the validation. First, muscle activation, which is simulation result of muscle, is compared with EMG (Electromyography) signals. The advantage of this method is that the individual muscles could be measured directly by EMG measuring devices. However, the disadvantage of this method is that it is difficult or impossible to measure all muscles.

Second method was to use the moment arm comparison. To validate the musculoskeletal model is possible by comparing the measured moment arm of muscles through the cadaver study and the calculated moment arm of muscles in simulation model. It is possible to compute the moment arm of the model's muscles and compare them to values from cadaver studies. In this research, the second method was used to validate the musculoskeletal model. [22]

The origin and the insertion points of muscles affect the moment arm of muscles. To determine the origin and the insertion points of muscles, a computational optimization method was used. This data-driven optimization method was used in [23]. The objective function used in the optimization was as follows.

$$\text{Minimize} \quad f(\vec{x}) = \sqrt{\sum_{i=1}^{m} \frac{[r_j(\vec{q_i}) - \widehat{r_j}(\vec{q_i}, \vec{x})]^2}{m}}$$

$$\text{Subject} \quad lb_j \leq x_j \leq ub_j$$

The objective function was the root mean square error between the predicted moment arms ($\widehat{r_j}(\vec{q_j}, \vec{x})$) calculated by the model and the moment arms ($r_j(\vec{q_i})$) from cadaver study. Through this optimization method, we found the optimal origin and insertion points that minimized the difference of moment arms in the joint angle (q_i). Boundary conditions ($lb_j \leq x_j \leq ub_j$) constrained the muscle from passing through the bone and the skin.

Chapter 4. Result

4.1 Comparison of kinematics data

The x, y, z coordinates were compared between motion capture markers and virtual markers after scaling process. As shown in Figure [6~12], trajectories of marker 1, 2 and 3 in the middle finger were compared. For marker 1 which was located on the distal phalanx, there was little difference in the distance of two markers. The maximum distance between two markers were 0.6 mm in the x−coordinate. However, in case of marker 2 and 3, the maximum distance was 5.41mm and 5.04mm respectively. Comparison of linear velocity and acceleration was also conducted for marker 2 and 3, because the linear velocity and acceleration of segments are used in the equations of motion. Equations of motion are as follows:

$$\tau = M(q)\ddot{q} + C(q, \dot{q}) + G(q) - F$$

Because there was little difference about position of marker 1, the marker 1 was not compared. For marker 2, the maximum differences of linear velocity and acceleration were 6.83mm/s and 35.9mm/s^2 in the z−coordinate. Marker 3 showed 3.82mm/s and 23.0mm/s^2 difference in the x−coordinate.

➢ Coordinates comparison – Marker 1

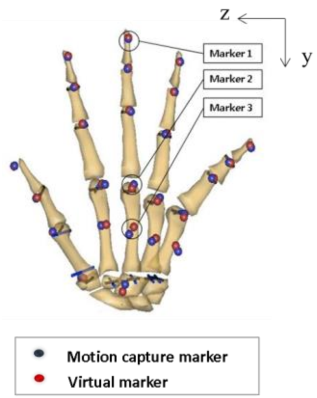

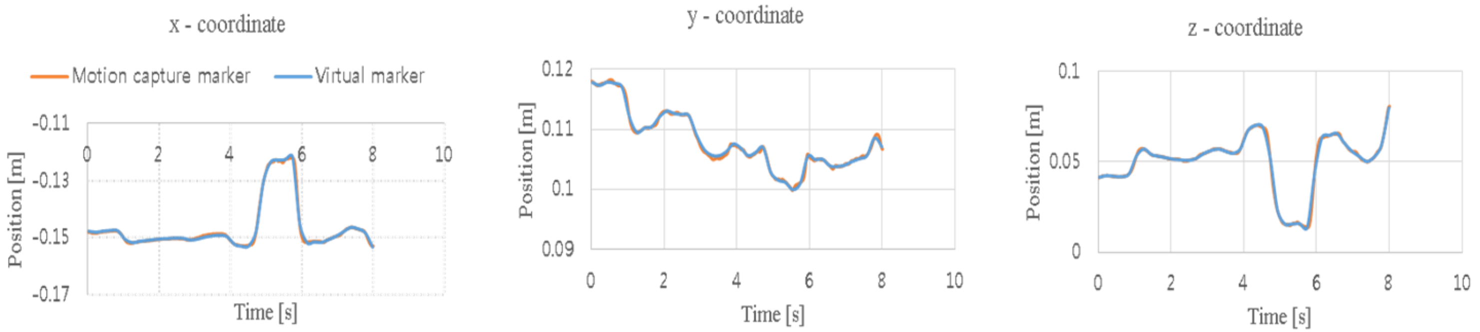

Maximum distance	X-coordinate	y-coordinate	Z-coordinate
Unit(mm)	**0. 6**	0.47	0.55

Figure 6. Coordinate comparison of marker 1 (Blue: motion capture marker, Orange: virtual marker)

➢ Coordinates comparison – Marker 2

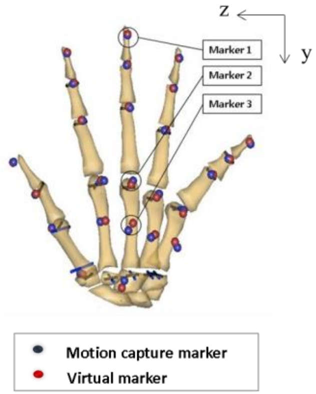

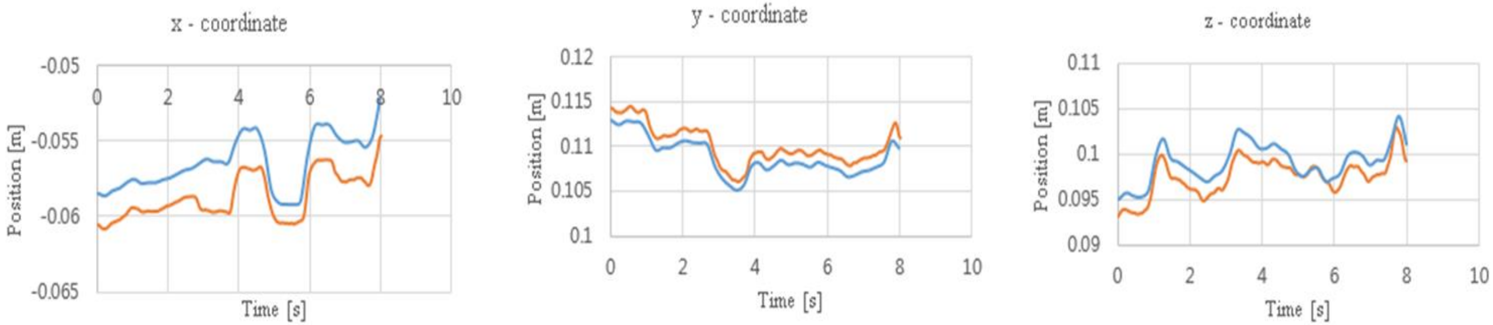

Maximum distance	X-coordinate	y-coordinate	Z-coordinate
Unit(mm)	**5.41**	2.49	1.50

Figure 7. Coordinate comparison of marker 2 (Blue: motion capture marker, Orange: virtual marker)

➢ Coordinates comparison – Marker 3

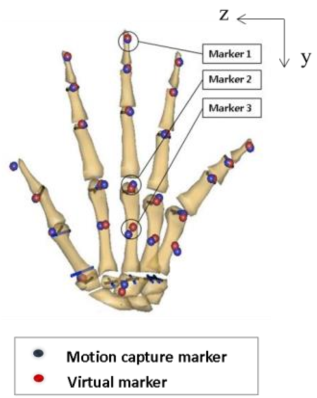

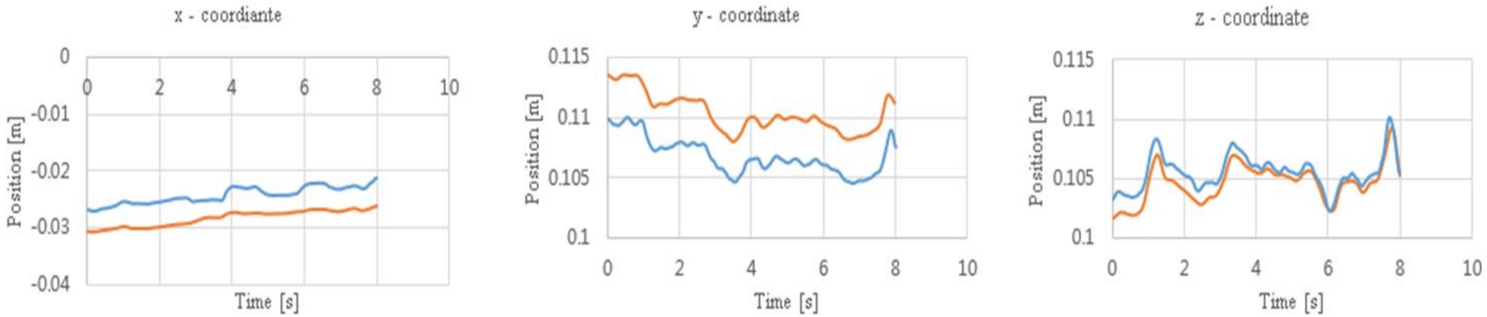

Maximum distance	X-coordinate	y-coordinate	Z-coordinate
Unit(mm)	**5.04**	3.84	1.74

Figure 8. Coordinate comparison of marker 3 (Blue: motion capture marker, Orange: virtual marker)

- Velocity comparison – Marker 2

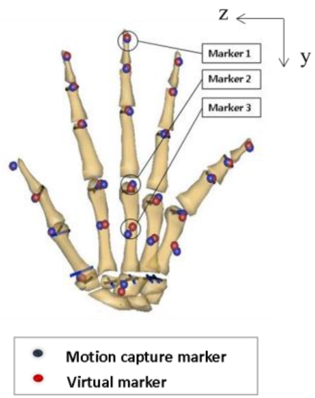

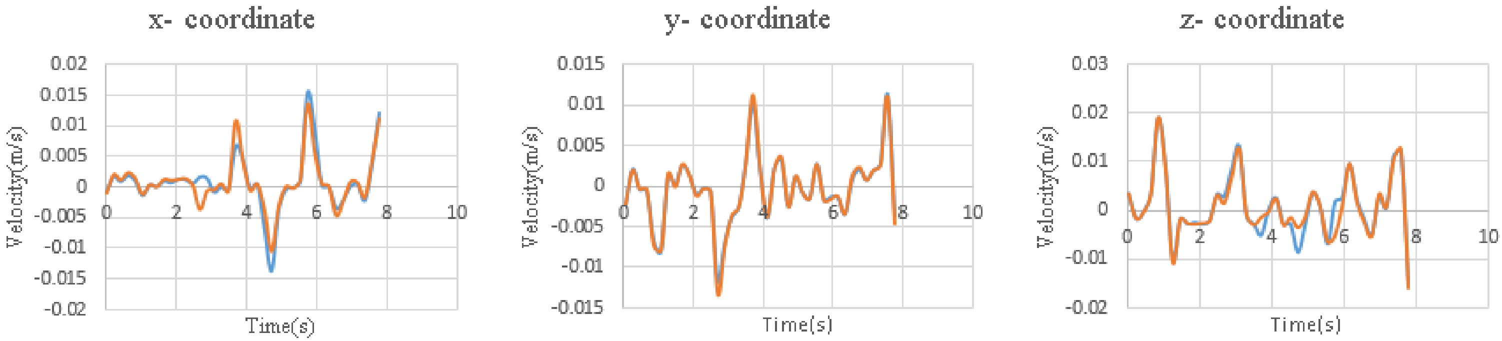

Maximum difference	X-coordinate	y-coordinate	Z-coordinate
Unit(mm/s)	5.41	1.73	**6.83**

Figure 9. Velocity comparison of marker 2(Blue: motion capture marker, Orange: virtual marker)

➢ Velocity comparison – Marker 3

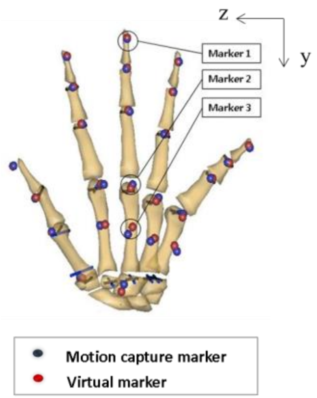

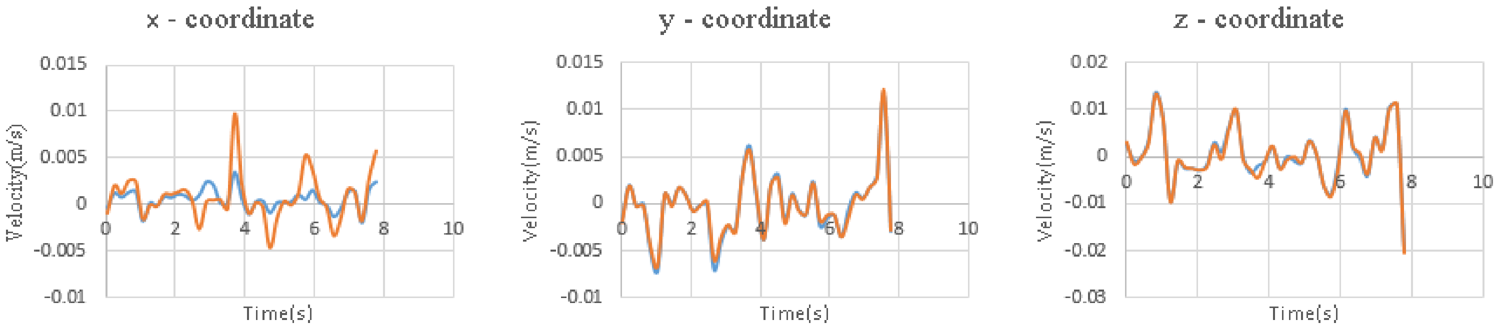

Maximum difference	X-coordinate	y-coordinate	Z-coordinate
Unit(mm/s)	**3.82**	0.79	2.49

Figure 10. Velocity comparison of marker 3(Blue: motion capture marker, Orange: virtual marker)

➢ Acceleration comparison – Marker 2

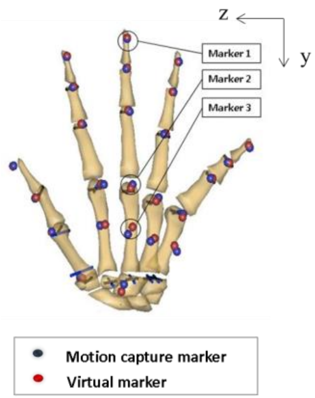

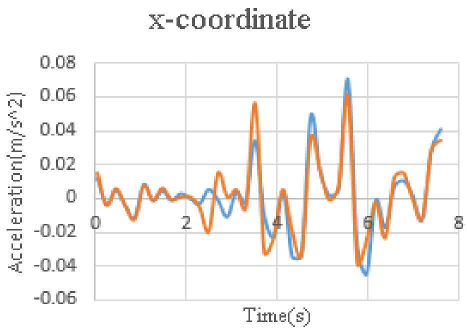

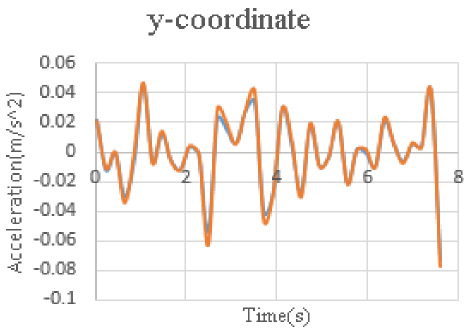

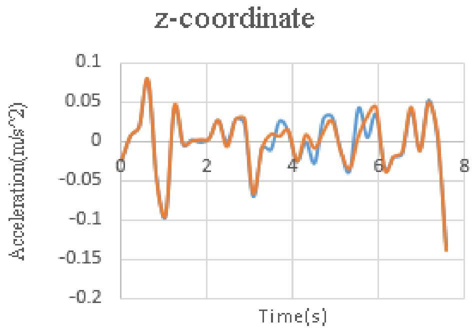

Maximum difference	X-coordinate	y-coordinate	Z-coordinate
Unit(mm/s^2)	24.9	8.70	**35.9**

Figure 11. Acceleration comparison of marker 2(Blue: motion capture marker, Orange: virtual marker)

- Acceleration comparison – Marker 3

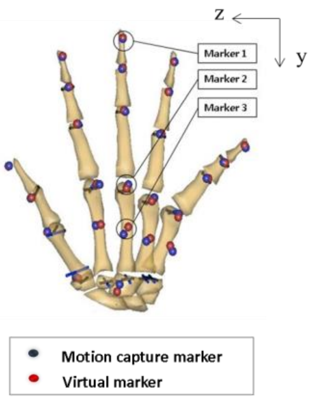

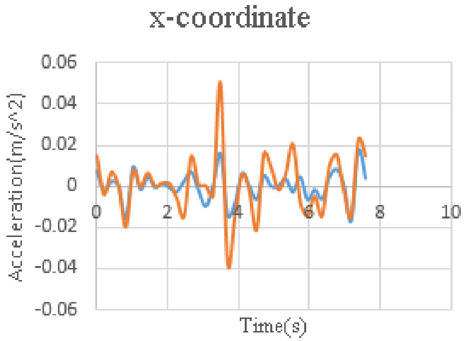

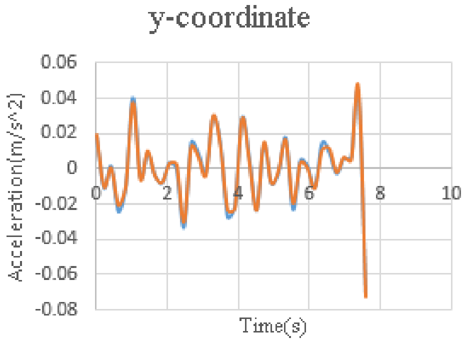

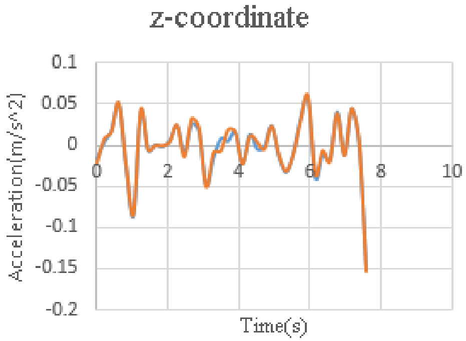

Maximum difference	X-coordinate	y-coordinate	Z-coordinate
Unit(mm/s^2)	**23.0**	3.94	1.50

Figure 12. Acceleration comparison of marker 3 (Blue: motion capture marker, Orange: virtual marker)

4.2 Comparison of muscle moment arms

To validate the muscle model of developed musculoskeletal model, the difference between experimentally-measured moment arms and calculated moment arms through the optimization method was analyzed. Six muscles of index finger, which were the 3 extrinsic muscles and the 3 intrinsic muscles, were compared, because experimental moment arm curves are available for the index finger at the MCP joint. Figure13 shows the moment arms during the MCP joint flexion of the index finger. To compare moment arms between experimentally-measured moment arms and calculated moment arms through optimization, coefficient of determination (R^2) and Root Mean Square Error were calculated. Coefficient of determination is the square of the correlation(r) between calculated moment arms and experimentally-measured moment arms. The coefficient of determination (R^2) ranges from 0 to 1 and an R^2 of 1 means that there is no difference between the two curves. Root Mean Square Error (RMSE) represents the standard deviation of the differences between moment arms. This value is always between

0 and 1. Coefficient of determination (R^2) was higher than 0.9 and RMSE was lower than 0.2 for 4 muscles (radial interossei (RI), lumbrical muscle (LU), flexor digitorum profundus (FP), flexor digitorum superficials (FS)). However, coefficient of determination (R^2) for extensor digitorum communis (EC) and ulnar interossei (UI) were 0.6910 and 0.5864, respectively.

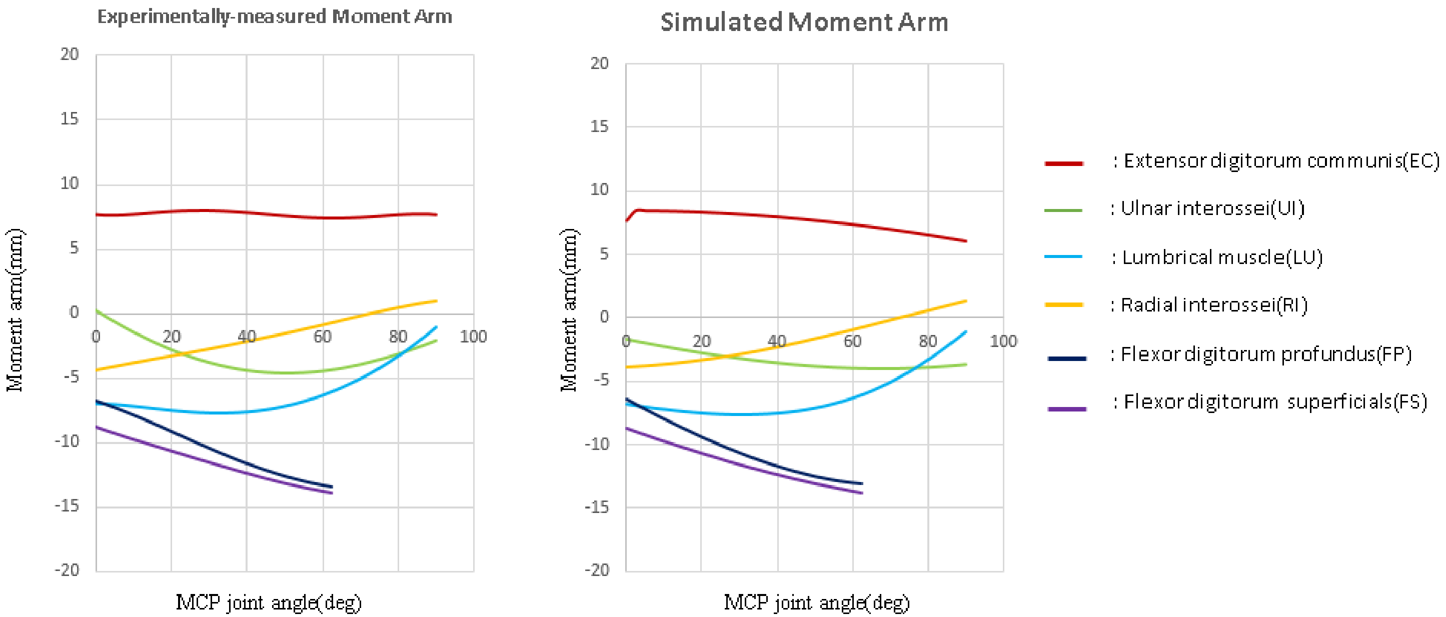

	RI	LU	FP	FS	EC	UI
R-square	0.9889	0.9993	0.9906	0.9991	0.6910	0.5864
RMSE	0.1714	0.0480	0.2062	0.0452	0.3404	0.8569

Figure 13. Moment arm comparison

Chapter 5. Discussion

The position, linear velocity, and linear acceleration were compared between motion capture markers and virtual markers attached to the musculoskeletal model. The result showed the less position difference for marker 1 than for marker 2 and 3. However, for velocity comparison of marker 2 and 3, the similarity between the curve of motion capture marker and the curve of the virtual marker was higher than the similarity between the curves for position comparison. It means that the positions of the virtual marker 2and 3 were not well-estimated. It is hard to estimate the accurate position of markers attached to the metacarpal bone. But, this problem could be solved using X-ray and computed tomography.

In the comparison of moment arms, the moment arms of four muscles (RI, LU, FP, and, FS) were well estimated through optimization method. However, the moment arms of two muscles (EC and UI) had quite high errors compared to the experimentally-measured moment arms. In this research, only muscle attachment points were considered to adjust moment arms. However, other factors such as a transition of joint axis, realistic joint type have to be considered for moment arms.

Chapter 6. Conclusion

The purpose of this study was to develop the hand musculoskeletal model using AnyBody Modeling System and validate the model. The skeletal hand model was created based on the anatomical data to implement degrees of freedom of hand. The musculoskeletal hand model included the hill-type muscle models which make hand movements. The origin and the insertion points of the muscles were founded using an optimization method to create moment arms of muscles from cadaveric study. The distance between motion capture markers and virtual markers was compared to validate the skeletal model. Muscles were validated through the comparison between the experimentally-measured moment arms of muscles and calculated moment arms of muscles in the musculoskeletal model. The developed hand musculoskeletal model could be used to analyze musculoskeletal diseases in the hand such as carpal tunnel syndrome. This study will help understanding of pathological causes and improving the pathological diagnosis.

Bibliography

[1] Winter, David A. Kinematics. John Wiley & Sons, Inc., 1990.

[2] Pandy, Marcus G. "Computer modeling and simulation of human movement. "Annual review of biomedical engineering 3.1 (2001): 245-273.

[3] Delp, Scott L., et al. "OpenSim: open-source software to create and analyze dynamic simulations of movement." Biomedical Engineering, IEEE Transactions on 54.11 (2007): 1940-1950.

[4] Anderson, Frank C., and Marcus G. Pandy. "Dynamic optimization of human walking." Journal of biomechanical engineering 123.5 (2001): 381-390.

[5] Pandy, Marcus G., and Thomas P. Andriacchi. "Muscle and joint function in human locomotion." Annual review of biomedical engineering 12 (2010): 401-433.

[6] Christophy, Miguel, et al. "A musculoskeletal model for the lumbar spine."Biomechanics and modeling in mechanobiology 11.1-2 (2012): 19-34.

[7] Delp, Scott L., and J. Peter Loan. "A computational framework for simulating and analyzing human and animal

movement." Computing in Science & Engineering 2.5 (2000): 46-55.

[8] Fregly, Benjamin J., et al. "Grand challenge competition to predict in vivo knee loads." Journal of Orthopaedic Research 30.4 (2012): 503-513.

[9] Jung, Yihwan, et al. "Dynamically adjustable foot-ground contact model to estimate ground reaction force during walking and running." Gait & Posture (2016).

[10] Jung, Yihwan, Cong-Bo Phan, and Seungbum Koo. "Intra-articular Knee Contact Force Estimation during Walking using Force-reaction Elements and Subject-specific Joint Model." Journal of biomechanical engineering (2015).

[11] Sancho-Bru, Joaquín L., et al. "A 3D biomechanical model of the hand for power grip." Journal of biomechanical engineering 125.1 (2003): 78-83.

[12] Damsgaard, Michael, et al. "Analysis of musculoskeletal systems in the AnyBody Modeling System." Simulation Modelling Practice and Theory 14.8 (2006): 1100-1111.

[13] Tubiana, Raoul; Thomine, Jean-Michel; Mackin, Evelyn (1998). Examination of the Hand and Wrist (2nd ed.). Taylor &

Francis. ISBN 978-1-85317-544-2.

[14] Marieb, Elaine N (2004). Human Anatomy & Physiology (Sixth ed.). Pearson PLC. ISBN 0-321-20413-1.

[15] Kingston, Bernard (2000). Understanding joints: a practical guide to their structure and function. Nelson Thornes. ISBN 0-7487-5399-0

[16] Gosling, J.A.; Harris, P.F.; Humpherson, J.R.; Whitmore, I.; Willan, P.L.T. (2008). Human Anatomy: Color Atlas and Textbook. phot. by A.L. Bentley (5th ed.). Philadelphia: Mosby. ISBN 978-0-7234-3451-0

[17] R. Al Nazer, A. Klodowski, T. Rantalanein, A. Heinonen, H. Sievänen, and A. Mikkola, Analysis of dynamic strains in tibia during human locomotion based on flexible multibody approach integrated with magnetic resonance imaging technique. Multibody System Dynamics, 20(4), 287-306, 2008.

[18] Hill, A. V. (1938). The heat of shortening and the dynamic constants of muscle. Proceedings of the Royal Society of London. Series B, Biological Sciences, 126(843), 136-195.

[19] Cordella, Francesca, et al. "Human hand motion analysis and synthesis of optimal power grasps for a robotic hand."

International Journal of Advanced Robotic Systems 11 (2014).

[20] Brand, R. A., Pedersen, D. R., & Friederich, J. A. (1986). The sensitivity of muscle force predictions to changes in physiologic crosssectional area. Journal of biomechanics, 19(8), 589-596.

[21] Andersen, Michael Skipper, et al. "A computationally efficient optimization-based method for parameter identification of kinematically determinate and over-determinate biomechanical systems." Computer methods in biomechanics and biomedical engineering 13.2 (2010): 171-183.

[22] An, Kai-Nan, et al. "Tendon excursion and moment arm of index finger muscles." Journal of biomechanics 16.6 (1983): 419-425.

[23] Lee, Jong Hwa, et al. "Extrinsic and intrinsic index finger muscle attachments in an opensim upper-extremity model." Annals of biomedical engineering 43.4 (2015): 937-948.

초 록

생체역학이란, 생체시스템을 이해하기 위해 역학적 원리를 이용하는 학문 분야이다. 생체역학 분야에서는 컴퓨터 모델링 및 시뮬레이션을 이용한 분석연구가 진행되어왔다. 실험을 통해 직접적으로 측정할 수 없었던 관절의 힘, 모멘트 및 근육힘을 근, 골격 시뮬레이션을 이용해 예측할 수 있다. 특히, 보행동작과 관련된 다양한 근, 골격 모델이 개발되고 이를 토대로 정확한 지면반력 및 무릎 관절 접촉력을 예측할 수 있게 되었다. 그러나, 상대적으로 인간의 상지 근, 골격 모델에 대한 개발 연구는 많이 진행되지 않았다. 실제로 상용 근, 골격 시뮬레이션 프로그램에서 검증된 상지 모델을 제공하지 않고 있다. 본 연구에서는 다양한 손 동작에 대한 생체역학적 분석을 위한 근, 골격 모델을 개발하고 검증하고자 하였다. 근, 골격 모델의 개발과 다자유도 동역학 해석을 위해 상용 프로그램인 AnyBody Modeling System(AMS)를 사용하였다. 골격 모델은 해부학 자료를 기반으로 다자유도 손모델을 구현하였으며 근육 모델은 생체역학에서 가장 널리 쓰이는 Hill-type 근육 모델이 사용되었다. 근육의 기시부와 종지부 위치를 찾기 위한 최적화 기법을 사용하여 사체 연구를 통해 얻어진 근육의 모멘트 암을 근, 골격 모델에서 얻고자 하였다. 개발된 근, 골격 모델에 대한 검증을

위해 움직이는 동안 모션 캡쳐 마커와 근, 골격 모델에 부착된 가상 마커의 위치 차이를 비교하였다. 근육 모델은 사체 연구를 통해 얻어진 모멘트 암과 근, 골격 모델에서 계산된 모멘트 암의 비교를 통해 검증되었다. 개발된 손 근, 골격 모델은 손목 터널 증후군과 같이, 손목 및 손 부분에서 생기는 근, 골격 질환에 대해서 생체역학적 분석을 이해하는데 도움을 주고 향후 본 연구를 통해 손의 병리학적 진단 및 개선을 위한 연구에도 도움을 줄 수 있을 것으로 기대된다.

키워드: 근, 골격 모델, 컴퓨터 시뮬레이션, 손, 모션 캡쳐, 모멘트 암, 검증

학 번: 2014-22506